PROCEEDINGS OF SPIE

SPIEDigitalLibrary.org/conference-proceedings-of-spie

# Amplifier limited information rates in high-speed optical fiber communication systems

Ji Qi, Tianhua Xu, Zheng Liu, Cenqin Jin, Tongyang Xu, et al.

Ji Qi, Tianhua Xu, Zheng Liu, Cenqin Jin, Tongyang Xu, Lingbo Li, Leslie Kanthan, Jian Zhao, Tiegen Liu, "Amplifier limited information rates in high-speed optical fiber communication systems," Proc. SPIE 12314, Optoelectronic Devices and Integration XI, 1231404 (20 December 2022); doi: 10.1117/12.2643394

Event: SPIE/COS Photonics Asia, 2022, Online Only

# Amplifier Limited Information Rates in High-Speed Optical Fiber Communication Systems

Ji Qi[a], Tianhua Xu*[abc], Zheng Liu[a], Cenqin Jin[b], Tongyang Xu[cd], Lingbo Li[e], Leslie Kanthan[e], Jian Zhao**[a], and Tiegen Liu [a]

[a]School of Precision Instruments and Opto-Electronics Engineering, Tianjin University, Tianjin 300072, China

[b]School of Engineering, University of Warwick, Coventry, CV4 7AL, United Kingdom
[c]Department of Electronic and Electrical Engineering, University College London, London WC1E 6BT, United Kingdom

[d]School of Engineering, Newcastle University, Newcastle upon Tyne, NE1 7RU, United Kingdom

[e]Turing Intelligence Technology Limited, London EC2Y 9AW, United Kingdom

## ABSTRACT

Due to the high transmission capacity, optical fiber systems have been extensively applied, as significant components, in the modern telecommunication infrastructure to meet the ever-increasing demand of data traffic. Optical amplifiers have been employed to amplify optical signals and to compensate for the transmission losses. They play a key role in relaying the signals in ultra-wideband optical fiber communication systems. However, the amplified spontaneous emission (ASE) noise will be introduced during such process, and it will degrade the performance of optical fiber systems and will pose constraints on the transmission information rates. The mutual information (MI) and the generalized mutual information (GMI) have been applied and investigated, as figures of merit, to evaluate the information rates in communication systems. The MI measures the highest achievable information rate (bits per symbol) that can be realized in a channel based on ideal symbol-wise encoder and decoder. The GMI, also known as the bit-interleaved coded modulation (BICM) capacity, indicates an upper bound on the number of bits per symbol that can be reliably transmitted through a channel based on the bit-wise decoding. Although the MI and the GMI are equal when the signal-to-noise ratio (SNR) tends to infinity, the MI is strictly higher than the GMI in any practical transmission scenarios. This discrepancy depends on the constellation cardinality and the binary labeling. In this work, we have investigated the impact of ASE noise on the MI and the GMI, and have developed corresponding analyses and estimations across different modulation formats, in linear optical fiber communication systems. Our work aims to explore the limit and requirements on optical amplifiers and to provide a comprehensive insight for the design of next-generation ultra-wideband optical fiber communication systems.

**Keywords:** Optical fiber communication systems, mutual information, generalized mutual information

## 1. INTRODUCTION

Optical fiber systems have been applied in the modern telecommunication infrastructure to meet the ever-growing demand for data rates. For currently deployed fiber systems, high-order modulation formats are one of the most popular schemes to realize the increase in data rates. With the use of high-order modulation formats, the sensitivity of systems decreases, which conflicts with the requirement of the error-free transmission. To meet this requirement, the use of more advanced forward error correction (FEC) becomes a potential solution. The combination of the FEC and high-order modulation

Further author information: (Send correspondence to Tianhua Xu and Jian Zhao)
Tianhua Xu: E-mail: tianhua.xu@ieee.org
Jian Zhao: E-mail: enzhaojian@tju.edu.cn

Optoelectronic Devices and Integration XI, edited by Xuping Zhang, Baojun Li, Changyuan Yu, Xinliang Zhang, Proc. of SPIE Vol. 12314, 1231404 · © 2022 SPIE · 0277-786X · doi: 10.1117/12.2643394

formats is called coded modulation (CM). CM schemes typically operate with soft-decision (SD) decoding, which provides soft information on the code bits.[1]

Achievable information rates provide an upper bound on the number of bits per symbol that can be reliably transmitted through the channel.[2] Hard-decision (HD) decoding performs well in optical fiber communication systems in the case of limited decoding complexity. Assuming the ideal interleaving, the achievable rate of the HD-FEC decoder can be completely determined by the pre-FEC bit-error-rate (BER).[3] However, for CM schemes using the SD decoding, there is no such relationship between. This is followed by SD-FEC decoders using the information about the bit reliability rather than the information about hard decisions.[4] Mutual information (MI) is the largest achievable information rate for SD-FEC decoders. Thus, it becomes a natural figure of merit to be considered in SD decoding systems. In optical fiber communication systems, MI has been used as the prediction of post-FEC BER, which has been proven to be more credible than the pre-FEC BER, and employed as a reference for the analytical state lower-bound estimate on the channel capacity.[5-7]

Bit-interleaved coded modulation (BICM) is one of the most pragmatic and popular approaches in CM. BICM is characterized by a suboptimal decoder, which operates on bits rather than symbols. This receiver structure is referred to as a bit-wise (BW) decoder. In BW decoders, the soft information of bits is calculated in a demapper, and then an SD-FEC decoder is used. As mentioned above, MI is the largest achievable rate for any SD-FEC decoder. For a BW decoder, this index should be the generalized mutual information (GMI). GMI is an achievable rate of BW decoders, but it has not been proven to be the largest achievable rate. Nevertheless, GMI has been shown to predict the performance of BW decoders very well.[8-10] Although the MI and the GMI are equal when the signal-to-noise ratio (SNR) tends to infinity, the MI is strictly higher than the GMI in any practical transmission scenarios.

Optical amplifiers have been employed in optical fiber systems to amplify optical signals and compensate for transmission losses. However, in the application of optical amplifiers, the negative effects of amplifier spontaneous emission (ASE) noise cannot be ignored. In this work, ASE noise limited achievable information rates (MI and GMI) for SD-FEC decoders in the context of next-generation ultra-wideband optical fiber communication systems are studied. Most especially, the calculation method for MI and GMI based on the Gauss-Hermite quadrature is provided. This allows us to quantify changes in information rates when system parameters or the digital signal processing (DSP) of the considered system are varied.

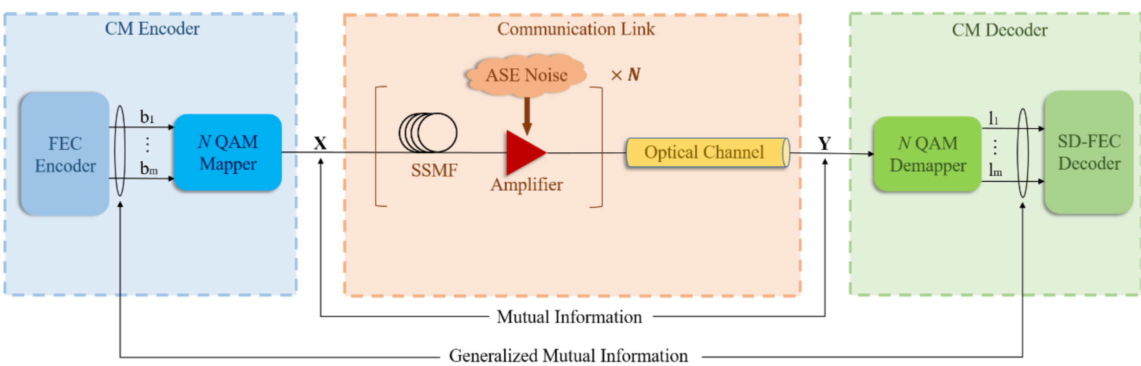


Figure 1. CM transceiver with SD-FEC under consideration. The transmitter consists of a binary FEC encoder followed by an *N*-QAM mapper. The receiver is a BW receiver, which is followed by an SD-FEC decoder.

## 2. SYSTEM MODEL AND ASE NOISE

### 2.1 System model

The CM transceiver we consider in this work is shown in Figure 1, which is popular in optical fiber communication systems.[11,12] A binary FEC encoder at the transmitter generates code bits $b_1, \ldots, b_m$, where $\boldsymbol{b}_k = [b_{1,k}, \ldots, b_{n_s,k}]$ for $k = 1, \ldots, m$ and $n_s$ is the number of transmitted symbols. Then a memoryless $N$-QAM mapper maps the code bits into a sequence of symbols $\boldsymbol{X} = [x_1, \dots, x_{n_s}]$, which are assumed to be multidimensional symbols with $M$ complex dimensions and uniformly drawn from a discrete constellation with cardinality $\mathbf{S} = \{s_1, \dots, s_N\}$, where $N = 2^n$ and probability mass function (PMF) $P_{\boldsymbol{X}}(x) = 1/N$. After the transmission over the communication link dominated by ASE noise, the received symbol sequence $\boldsymbol{Y} = [y_1, \dots, y_{n_s}]$ is processed by a CM decoder, which provides the soft information of the transmitted information sequence.[13-15] The difference between the two symbols is defined as the vector $d_{i,j} = x_i - x_j$. In this work, we consider the most common case in optical fiber communication systems, which is $M = 2$, corresponding to coherent communication using two polarizations of the optical signal.[16]

The optical channel in Figure 1 includes all transmitter-side digital signal processing (DSP) used after the $N$-QAM mapper, i.e., pulse shaping, polarization multiplexing, etc., and receiver-end DSP, i.e., digital backpropagation, matched filtering, etc.[17]

### 2.2 ASE noise

In an optical amplifier, the activated photons return to the ground state from the excited state and amplify the optical signal. Simultaneously, random incoherent spontaneous emission of the excited photons will be generated, which is the source of the amplified spontaneous emission (ASE) noise. To facilitate the analysis, we discuss the most commonly used Erbium-doped fiber amplifier (EDFA). In typical EDFA with bandwidth $B_0$, the power of the ASE noise can be expressed as[18]

$$P_{ASE} = 2n_{sp}\mathrm{h}\vartheta(\mathrm{G}-1)B_0 \tag{1}$$

where $n_{sp}$ is the noise factor, of which the typical value is 1~4, $h$ is the Planck constant, $\vartheta$ is the frequency of the optical signal and $G$ is the gain of the amplifier. The generation of ASE noise will pose constraints on the signal-to-noise ratio (SNR), thus, restricting the achievable information rates. In the next-generation long-haul ultra-wideband optical fiber communication systems, the increase of ASE noise caused by the expansion of the bandwidth, and the cumulative effect induced by the cascade use of amplifiers will affect the performance of communication systems seriously.

Since the ASE noise is additive, we equivalent the ASE noise dominated channel in the model shown in Figure 1 to a discrete-time, memoryless, vectorial AWGN channel

$$Y_n = X_n + Z_n \tag{2}$$

where, $X_n$, $Y_n$, $Z_n$ are real vectors and $n = 1, \dots, n_s$is the discrete-time parameter. The noise vector $Z_n$ is an independent zero-mean Gaussian random variable with a variance of $N_0/2$. Thus,

$$f_{Y_n \mid X_n}(y|x) = \frac{1}{(\pi N_0)^2} \exp\left(-\frac{\|y-x\|^2}{N_0}\right) \tag{3}$$

## 3. ACHIEVABLE RATE ANALYSES

### 3.1 Mutual information

Given that the transmitted symbol sequence is $\boldsymbol{X}$ and the received symbol sequence is $\boldsymbol{Y}$, for memoryless channels, the MI is defined as

$$I(\boldsymbol{X};\boldsymbol{Y}) = E_{\boldsymbol{X},\boldsymbol{Y}}[log_2 \frac{f_{\boldsymbol{Y} \mid \boldsymbol{X}}(y|x)}{f_{\boldsymbol{Y}}(y)}] \tag{4}$$

Where $E_{X,Y}$ denotes the expectation about $X$ and $Y$. The MI $I(X;Y)$ represents the information content in bits per symbol about $X$ that is included in $Y$.

For a given discrete constellation S, the MI in (7) can be also expressed as

$$I(\boldsymbol{X};\boldsymbol{Y}) = \frac{1}{N}\sum_{i=1}^{N}\int_{\boldsymbol{S}} f_{\boldsymbol{Y} \mid \boldsymbol{X}}(y|x)\, log_2 \frac{f_{\boldsymbol{Y} \mid \boldsymbol{X}}(y|x)}{\frac{1}{N}\sum_{j=1}^{N} f_{\boldsymbol{Y} \mid \boldsymbol{X}}(y|x)} dy \tag{5}$$

The operation meaning of the MI is that, for given channels and a fixed PMF, only when the system transmits under this rate, coding schemes that allow the post-FEC BER to be arbitrarily small exist. Higher information rates demand varying channels or the PMF.

### 3.2 Generalized mutual information

For the BW decoder in Figure 1, an achievable rate is the GMI, which indicates an upper bound on the number of bits per symbol that can be reliably transmitted in the BICM system. The GMI is defined as

$$G = \sum_{k=1}^{m} I(\boldsymbol{b_k}; \boldsymbol{Y}) \tag{6}$$

Where

$$I(\boldsymbol{b_k}; \boldsymbol{Y}) = E_{\boldsymbol{b_k},\boldsymbol{Y}}[\log_2 \frac{f_{\boldsymbol{Y} \mid \boldsymbol{b_k}}(\boldsymbol{Y} \mid \boldsymbol{b_k})}{f_{\boldsymbol{Y}}(y)}] \tag{7}$$

Based on the operating principle of the *N*-QAM demapper in Figure 1, it can be deduced that $I(\boldsymbol{b}; \boldsymbol{Y}) = I(\boldsymbol{X}; \boldsymbol{Y})$. Hypothesizing independent bits, the chain rule of MI[19] gives

$$I(\boldsymbol{b}; \boldsymbol{Y}) \geq \sum_{k=1}^{m} I(\boldsymbol{b_k}; \boldsymbol{Y}) \tag{8}$$

Thus

$$I(\boldsymbol{X}; \boldsymbol{Y}) \geq G \tag{9}$$

The difference between MI and GMI can be regarded as the expense in terms of achievable information rates caused by using the BW decoders, which is suboptimal. The rate expense is known to be small for Gray-labeled constellations.[20] Moreover, the GMI, unlike the MI, is highly dependent on the binary labeling.[21]

## 4. COMPUTATIONS OF ACHIEVABLE RATES

MI and GMI can be computed by using Gauss-Hermite quadrature and Monte-Carlo integration. When the channel law is unknown or the dimensionality of the constellation is large, Monte Carlo integration is preferred. However, compared with Monte-Carlo integration, the evolution of Gauss-Hermite quadrature does not depend on random samples, making it better suited for numerical optimizations[22]. Besides, Gauss-Hermite quadrature has lower complexity when applied to constellations with low complex dimensions, therefore, is normally faster when used for the ASE noise dominated optical channel we consider in this paper. The computation method based on the Gauss-Hermite quadrature is described in this section.

For any real-valued function $g(r)$ with bounded 2*J*-th derivative, the *J*-point Gauss-Hermite quadrature is given by[23]

$$\int_C \exp(-|r|^2) g(r) dr \approx \sum_{j_1=1}^{J} \alpha_{j_1} \sum_{j_2=1}^{J} \alpha_{j_2}\, g(\xi_{j_1} + j\xi_{j_2}) \tag{10}$$

Where the quadrature nodes $\xi_j$ and the weights $\alpha_j$ can be easily obtained for different $J$ values. The $J$ value determines the tradeoff between the accuracy and the computation speed.

Using the method of Gauss-Hermite quadrature, the MI and the GMI for the ASE noise dominated channel can be approximated as[24, 25]

$$I(\boldsymbol{X}; \boldsymbol{Y}) \approx m - \frac{1}{N\pi} \sum_{i=1}^{N} \sum_{j_1=1}^{J} \alpha_{j_1} \sum_{j_2=1}^{J} \alpha_{j_2} \log_2 \sum_{j=1}^{N} \exp(-2 \frac{|d_{i,j}|^2 + \sqrt{2N_0} R\{(\xi_{j_1} + j\xi_{j_2}) d_{i,j}\}}{N_0}) \tag{11}$$

and

$$G \approx m - \frac{1}{N\pi} \sum_{k=1}^{m} \sum_{b \epsilon \{0,1\}} \sum_{i \epsilon L^b{}_k} \sum_{j_1=1}^{J} \alpha_{j_1} \sum_{j_2=1}^{J} \alpha_{j_2} \log_2 \frac{\sum_{p=1}^{N} \exp(-2\frac{|d_{i,p}|^2 + \sqrt{2N_0} R\{(\xi_{j_1} + j\xi_{j_2}) d_{i,p}\}}{N_0})}{\sum_{j \epsilon L^b{}_k} \exp(-2\frac{|d_{i,j}|^2 + \sqrt{2N_0} R\{(\xi_{j_1} + j\xi_{j_2}) d_{i,j}\}}{N_0})} \tag{12}$$

where $L^b{}_k \in \{1,2, \ldots, N\}$ with $|L^b{}_k| = N/2$ is the set of indices of constellation points of which the binary label is $b$ at the bit position $k$.

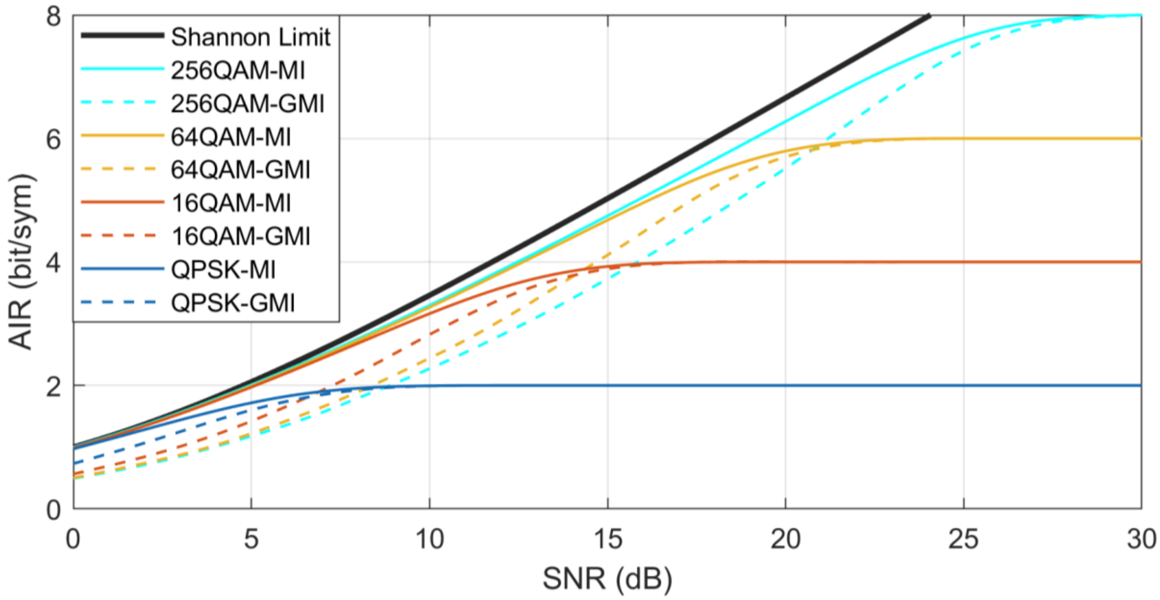


Figure 2. MI and GMI vs. SNR for the ASE noise dominated channel. The MI and GMI are calculated using (11) and (12) respectively. The Shannon limit is given by (13).

The MI and GMI for *N*-QAM constellations over the ASE noise dominated channel are shown in Figure 2, the binary labeling of GMI is the Gray code. The Shannon limit of the ASE noise dominated channel is

$$C = log_2(1 + SNR) \tag{13}$$

Given that the Gray code is used as the binary labeling, the GMI is very close to the MI when the SNR is high. This means the rate expense introduced by using BW decoders is very small. With further observation of Figure 2, it is noted that there is a range of SNR, in which an *N*-QAM modulation format with a smaller *N* has higher GMI than QAMs with larger cardinalities. This case is owned by the use of suboptimal BW decoders, and thus, does not appears for the MI.

## 5. CONCLUSIONS

In this paper, we analyzed the amplifier limited achievable information rates (the MI and GMI) in high-speed optical fiber communication systems. The approximations of the MI and GMI based on the Gauss-Hermite quadrature are represented and discussed. This work is focused on the ASE noise dominated channel, which is very relevant to optical transceivers used in next-generation ultra-wideband optical fiber communication systems.

The method based on the Gauss-Hermite quadrature described in this paper is advantageous for constellations with low dimensions, which is typical in optical communication systems. However, when the dimension grows and the channel law is unknown, Monte-Carlo integration is better suited. All the analyses were presented based on infinite-block length assumptions and universal codes. Discussions on both finite-block length and code universality are left for further investigations.

## ACKNOWLEDGEMENTS

This work is supported by National Key Research and Development Program of China 2022YFE0202100, EU Horizon 2020 MSCA Grant 101008280, and UK EPSRC Grant EP/S028455/1.

## REFERENCES


[1] A. Alvarado, and E. Agrell, "Four-dimensional coded modulation with bit-wise decoders for future optical communications," Journal of Lightwave Technology, 33(10), 1993-2003 (2015).

[2] T. Fehenberger, A. Alvarado, P. Bayvel et al., "On achievable rates for long-haul fiber-optic communications," Optics Express, 23(7), 83-91 (2015).

[3] T. Mizuochi, "Recent progress in forward error correction and its interplay with transmission impairments," IEEE Journal of Selected Topics in Quantum Electronics, 12(4), 544-554 (2006).

[4] A. Leven, F. Vacondio, L. Schmalen et al., "Estimation of soft FEC performance in optical transmission experiments," IEEE Photonics Technology Letters, 23(20), 1547-1549 (2011).

[5] M. P. Yankov, D. Zibar, K. J. Larsen et al., "Constellation shaping for fiber-optic channels with QAM and high spectral efficiency," IEEE Photonics Technology Letters, 26(23), 2407-2410 (2014).

[6] T. H. Xu, G. Jacobsen, S. Popov et al., "Analytical BER performance in differential n-PSK coherent transmission system influenced by equalization enhanced phase noise," Optics Communications, 334, 222-227 (2015).

[7] P. Poggiolini, G. Bosco, A. Carena et al., "The GN-model of fiber non-linear propagation and its applications," Journal of Lightwave Technology, 32(4), 694-721 (2014).

[8] P. Fertl, J. Jalden, and G. Matz, "Performance assessment of MIMO-BICM demodulators based on mutual information," IEEE Transactions on Signal Processing, 60(3), 1366-1382 (2012).

[9] A. Alvarado, F. Brannstrom, and E. Agrell, "A simple approximation for the bit-interleaved coded modulation capacity," IEEE Communications Letters, 18(3), 495-498 (2014).

[10] A. Alvarado, H. Carrasco, R. Feick et al., "On adaptive BICM with finite block-length and simplified metrics calculation," IEEE Vehicular Technology Conference Proceedings. 1893-1897 (2006).

[11] T. Xu, N. A. Shevchenko, Y. Zhang et al., "Information rates in Kerr nonlinearity limited optical fiber communication systems," Optics Express, 29(11), 17428-17439 (2021).

[12] A. Alvarado, E. Agrell, D. Lavery et al., "Replacing the soft-decision FEC limit paradigm in the design of optical communication systems," Journal of Lightwave Technology, 33(20), 4338-4352 (2015).

[13] C. Jin, N. A. Shevchenko, Z. Li et al., "Nonlinear coherent optical systems in the presence of equalization enhanced phase noise," Journal of Lightwave Technology, 39(14), 4646-4653 (2021).

[14] J. Ding, T. Liu, T Xu et al., "Intra-channel nonlinearity mitigation in optical fiber transmission systems using perturbation-based neural network," Journal of Lightwave Technology, doi: 10.1109/JLT.2022.3200827(2022).

[15] J. Cho, and P. J. Winzer, "Probabilistic constellation shaping for optical fiber communications," Journal of Lightwave Technology, 37(6), 1590-1607 (2019).

[16] Z. Qiao, Z. Y. Wan, G. Q. Xie et al., "Multi-vortex laser enabling spatial and temporal encoding," PhotoniX, 1(1): 13 (2020).

[17] J. Zhao, Y. P. Liu, and T. H. Xu, "Advanced DSP for coherent optical fiber communication," Applied Sciences, 9(19), 4192-4211 (2019).

[18] C. Stihler, C. Jauregui, S. E. Kholaif et al., "Intensity noise as a driver for transverse mode instability in fiber amplifiers," PhotoniX, 1(1): 8 (2020).

[19] T. Cover, and J. Thomas, [Elements of Information Theory, 2nd ed], Wiley, New York, 23-24 (2006).

[20] A. Alvarado, F. Brannstrom, E. Agrell et al., "High-SNR asymptotics of mutual information for discrete constellations with applications to BICM," IEEE Transactions on Information Theory, 60(2), 1061-1076 (2014).

[21] E. Agrell, and A. Alvarado, "Optimal alphabets and binary labelings for BICM at low SNR," IEEE Transactions on Information Theory, 57(10), 6650-6672 (2011).

[22] A. Alvarado, T. Fehenberger, B. Chen et al., "Achievable information rates for fiber optics: applications and computations," Journal of Lightwave Technology, 36(2), 424-439 (2018).

[23] R. F. Churchhouse, [Handbook of Applicable Mathematics, vol 3], Wiley, New York, 365 (1981).

[24] T. A. Eriksson, T. Fehenberger, P. A. Andrekson et al., "Impact of 4D channel distribution on the achievable rates in coherent optical communication experiments," Journal of Lightwave Technology, 34(9), 2256-2266 (2016).

[25] E. Sillekens, A. Alvarado, C. M. Okonkwo et al., "An experimental comparison of coded modulation strategies for 100 Gb/s transceivers," Journal of Lightwave Technology, 34(24), 5689-5697 (2016).